SKB

TECHNICAL REPORT 90-31

Near-field performance of the advanced cold process canister

Lars Werme

Swedish Nuclear Fuel and Waste Management Co
(SKB)

September 1990

SVENSK KÄRNBRÄNSLEHANTERING AB
SWEDISH NUCLEAR FUEL AND WASTE MANAGEMENT CO

BOX 5864 S-102 48 STOCKHOLM

TEL 08-665 28 00 TELEX 13108 SKB S
TELEFAX 08-661 57 19

NEAR-FIELD PERFORMANCE OF THE ADVANCED COLD PROCESS CANISTER

Lars Werme

Swedish Nuclear Fuel and Waste Management Co (SKB)

September 1990

NEAR-FIELD PERFORMANCE OF THE ADVANCED COLD PROCESS CANISTER

Lars Werme
Swedish Nuclear Fuel and Waste Management Co. (SKB)
Stockholm, Sweden

ABSTRACT

A near-field performance evaluation of an Advanced Cold Process Canister for spent fuel disposal has been performed jointly by TVO, Finland and SKB, Sweden. The canister consists of a steel canister as a load bearing element, with an outer corrosion shield of copper. The canister design was originally proposed by TVO. In the analysis, as well internal (ie corrosion processes from the inside of the canister) as external processes (mechanical and chemical) have been considered both prior to and after canister breach. Throughout the analysis, present day underground conditions has been assumed to persist during the service life of the canister.

The major conclusions for the evaluation are:

Internal processes cannot cause the canister breach under foreseen conditions, ie localized corrosion for the steel or copper canisters can be dismissed as a failure mechanism.

The evaluation of the effects of processes outside the canister indicate that there is no rapid mechanism to endanger the integrity of the canister. Consequently the service life of the canister will be several million years. This factor will ensure the safety of the concept.

For completeness also evaluation of post-failure behaviour was carried out. Analyses were focussed on low probability phenomena from faults in canisters.

Some items were identified where further research is justified in order to increase knowledge of the phenomena and thus strengthen the confidence of safety margins. However, it can be concluded that the risks of these scenarios can be judged to be acceptable. This is due to the fact that firstly, the probability of occurrence of most of these scenarios can be controlled to a large extent through technical measures. Secondly, these analyses indicated that the consequences would not be severe.

As a summary, according to this evaluation the Advanced Cold Process Canister seems to meet at least the same safety targets as the KBS-3 canister.

TABLE OF CONTENT

1 INTRODUCTION

1.1 Background

Work on the development of a cold process for encapsulation of spent fuel has been in progress at TVO since 1987. The purpose of the studies was to define a method for encapsulation in which elevated temperatures were not required for producing a copper canister of sufficient structural stability. Recently, some doubts has been thrown upon the ductility of copper under creep deformation. Due to these uncertainties, TVO has made an alternative canister design; a copper canister with an inner carbon steel support [Salo & Raiko]. During 1989, also SKB has developed an active interest in cold process canister designs and in particular in the copper/steel composite canister as well as in an evaluation of its performance in a KBS-3 type repository for spent nuclear fuel. Therefore, TVO and SKB has decided to jointly evaluate the near field performance of a composite copper/steel canister in a repository.

1.2 Aim of present study

The objective of the study reported here is to identify and describe relevant events and processes in the near field and to make an evaluation of pre-failure and post-failure scenarios for the case when the present geological and hydrological situation in Scandinavia is prevailing.

Throughout the study, a situation as described in KBS-3 has been assumed to prevail and data from the KBS-3 evaluation have been used where no deviation from the KBS-3 scenarios has been identified or when recent research has not presented any grounds for a re-evaluation of the KBS-3 scenario. Thus, scenarios and processes

which are common to both concepts have not, in general, been addressed in this analysis, except when necessary for the completeness of the corrosion evaluation.

2 CANISTER DESIGN

The preliminary designs and evaluations of the two alternative canisters to be considered are described in Salo & Raiko. The principle is in both cases a double canister system, where the spent nuclear fuel bundles are packed into an inner steel canister providing structural support to an outer corrosion resistant canister of oxygen free high conductivity (OFHC) copper. One alternative, case 1, has the wall thicknesses of 55 mm for steel and 60 mm for copper shell (Fig. 1), while the other alternative, case 2, has the wall thicknesses of 50 mm for steel and 50 mm for copper (Fig. 2). The principle difference between the two designs is that in case 1, the desired radiation level is achieved through the choice of wall thicknesses at the expense of increased canister dimensions. In case 2, this is achieved through an extra lead liner inside the canister. The mechanical dimensioning of the combined copper/steel canister is made according to Finnish standards (SFS) for pressure vessels. All essential strength and dimensioning aspects are reported in Salo & Raiko together with full design details.

In order to reduce the void volume inside the canister, it will be partially filled with particulate matter, such as lead shots, glass beads, quartz sand or magnetite. Together with the volume of the fuel elements, the resulting void volume is about 35%. This residual volume will be either ambient (hot cell) air or a suitable inert gas, such as argon.

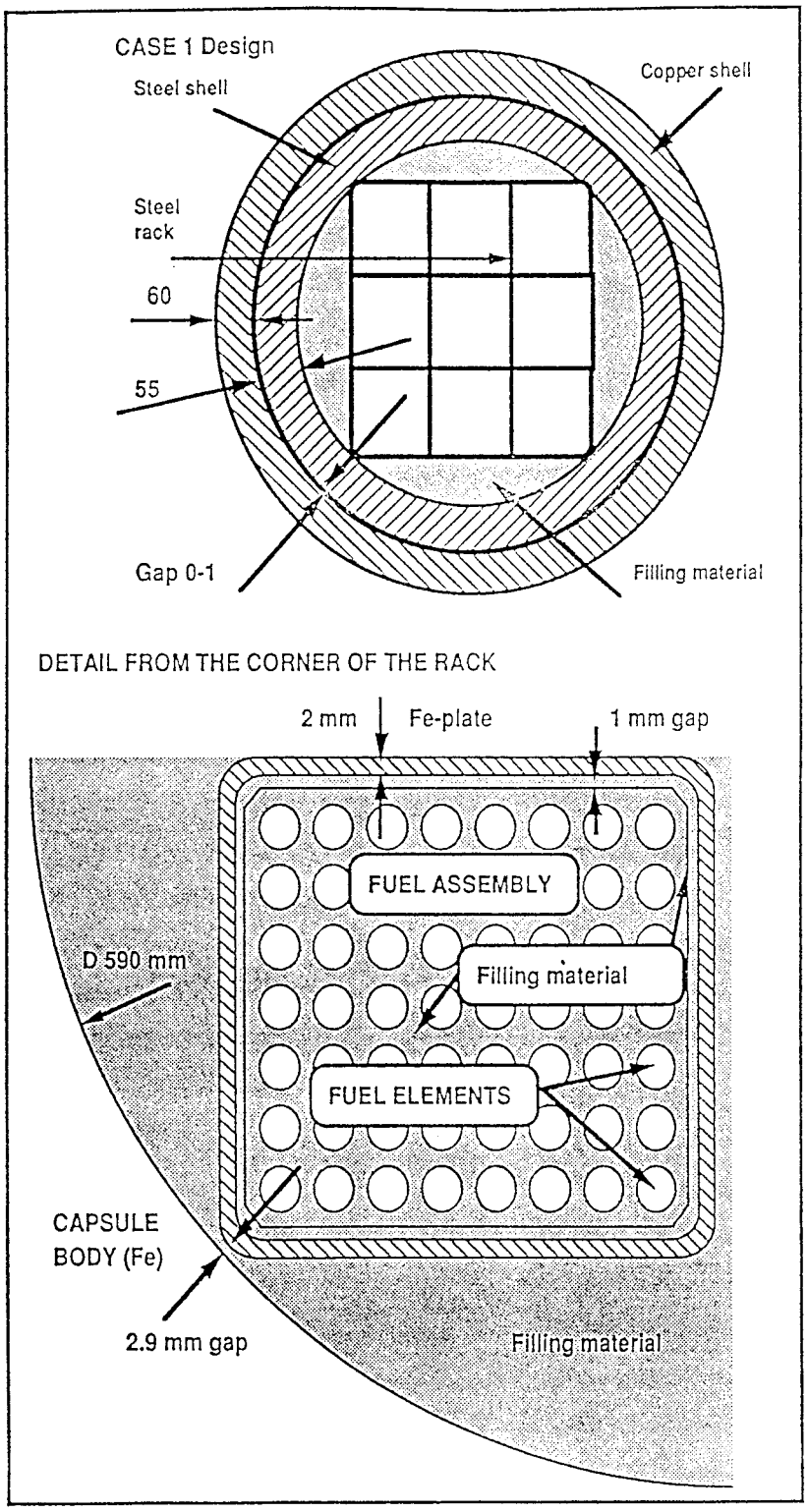

Figure 1: Canister design, case 1.

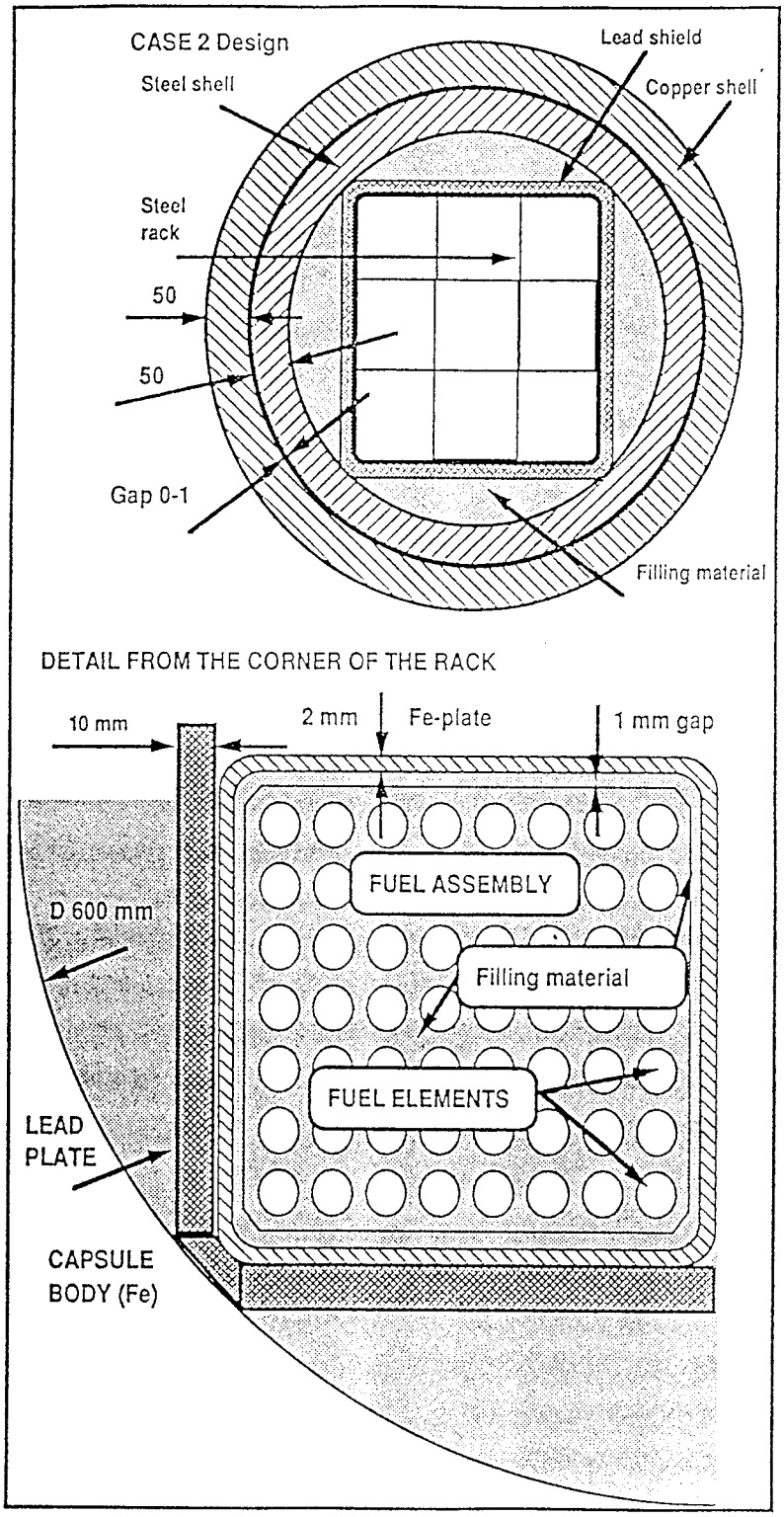

Figure 2: Canister design, case 2.

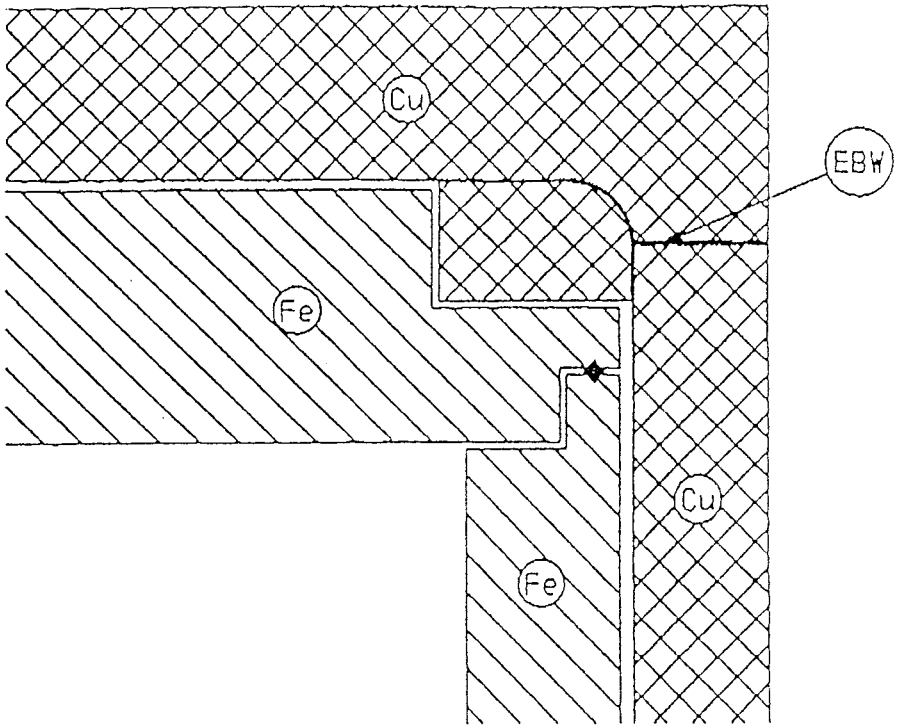

Figure 3: Proposed lid configuration.

The outer copper shell is to be sealed using electron beam (EB) welding [Sanderson et al.]. This procedure requires some special considerations for ensuring maximum possible integrity of EB weld. A proposed lid design is shown in Figure 3. The basic features of this design are:

1) The EB weld is placed at a position where it can be most easily non destructively tested.
2) There is a substantial quantity of copper backing to easily avoid penetration into the steel canister and possible subsequent steel pick up in the weld.
3) The EB weld is placed in a position of moderate stress concentrations.
4) The inner steel canister is sealed using a gas tight gasket in order to avoid gases to reach the weld zone during welding. For the same reasons,

and also to avoid excessive pumping, the narrow gap between the steel canister and the copper canister is also sealed.

Neither of these measures are considered to affect in any way the performance of the canister after disposal.

3 REFERENCE SCENARIO

The spent fuel canisters are deposited in a KBS-3 type repository in such a way that the temperature on the outer surface of the canister never exceeds 100°C. The maximum radiation level at the canister surface is estimated to be about 100 mSv/h. After water saturation of the repository the external pressure will reach a value of 15 MPa resulting from a hydrostatic pressure of 5 MPa and a bentonite swelling pressure of a maximum of 10 MPa. The water flow is assumed to be 10 dm^3/canister·year. This is approximately the same value as used in the KBS-3 analysis, where water flow rates in the range 0.1 to 1 $dm^3 \cdot m^{-2} \cdot a^{-1}$ were discussed. Two scenarios are proposed for the water flow; one major fracture, or alternatively, 10 smaller fractures evenly distributed, per deposition hole. The composition of the groundwater is shown in Table I.

Table I. Assumed composition of the groundwater in the near-field. Estimates are made on the basis of the preliminary field investigation and the bentonite/water interaction tests.

pH		6.5...9.0
Eh(V)		-0.5...0
HCO_3^-	mg/l	40..500
SO_4^{2-}	"	40...60
HS^-	"	0.1...1
HPO_4^{2-}	"	0.1...0.2
PO_4^{3-}	"	0.01..1
NO_3^-	"	0.01..0.6
NO_2^-	"	0.01..0.1
Cl^-	"	1..17000
F^-	"	0.2..10
Ca^{2+}	"	5...3200
Mg^{2+}	"	1...50
Fe^{2+}	"	0.1...3
Fe^{3+}	"	$< 10^{-1}$
Mn^{2+}	"	0.2...0.5
K^+	"	1...25
Na^+	"	10...4000
Al^{3+}	"	0.01...0.2
SiO_2	"	2...20
TOC	"	1...8

4 PROCESSES BEFORE CANISTER BREACH

4.1 Processes inside canister

Measures will be taken to ensure that the interior of the canister is dry. However, the void volume of the canister will be filled with air with a typical relative humidity of 60 - 80 %. However, some water carry-over may occur with the fuel elements and the relative

humidity may rise to 100 % (at ambient temperature). This corresponds to, conservatively, 8 to 11 g of water if the canister is filled with particulate matter (and ca 20 g if the canister is empty). If this water reacts exclusively with the steel vessel, the depth of attack will be less than 1 μm. This is insignificant for the structural integrity of the canister. The entrapped oxygen in the canister is approximately 4 mols and 10 mols, respectively, for the two cases. Steel is very inert in air even at 150 ^{o}C and the oxidation rate is expected to be slow. Stoichiometrically, however, these values correspond to a general corrosion in the order 10 μm, which, again, is insignificant [Marsh].

In the intense gamma-field inside the canister, there will be some radiolytic production of nitrous and nitric acids. However, the rate of radiolytic production will be relatively slow and the amounts of acid produced will ultimately be limited by the availability of nitrogen, oxygen and water. Assuming 10 g of water inside the canister and a constant water pressure, it will require 30 years for all water inside the canister to be converted into nitric acid. At such production rates, the corrosion inside the canister will have to be very slow if it is not to consume all available water before it can be transformed into HNO_3. Thus, localized corrosion such as crevice corrosion and stress corrosion cracking can be dismissed as failure mechanisms for the steel canister [Marsh]. Furthermore, the real situation in a closed canister would lead to a general drop in the water vapour pressure as the water is consumed in the acid formation. If this effect is considered, calculations show that the process of converting 10 g of water to 60 to 70 g nitric acid may take 140 years. [Henshaw el al.]. The unintentional transfer of substantially greater volumes of liquid water to the canister is unlikely. The Swedish fuel transport system employs dry transport casks. This is

accomplished by vacuum drying the fuel prior to loading and the safety report for the cask is based on the assumption that no liquid water will be transferred into the cask [Transnucléaire].

Calculations have also been performed to illustrate the effect of larger quantities of water. It was found that the amount of nitric acid produced increased to up to 150 g for about 30 g of initial water. After that the oxygen initially present limited the amount of acid produced. It was assumed that no other process, such as corrosion of the steel, was competing in the consumption of the water and oxygen. The time to produce the maximum quantity of nitric acid was 460 years [Henshaw et al.]. Again, at such production rates, the corrosion inside the canister will have to be very slow if it is not to consume all available water before it can be transformed into HNO_3. Thus, localized corrosion such as crevice corrosion and stress corrosion cracking can be dismissed as failure mechanisms for the steel vessel also in the case when larger quantities of water are transferred to canister.

Radiolysis of the water and corrosion of steel will lead to production of hydrogen. If the prevailing gas mixture inside the canister consists of nitrogen and hydrogen, there is a possibility for radiolytic production of ammonia. Calculations have shown that for 10 g initial water, 4.5 g of ammonia will be produced after some 200 years. The rate of ammonia production increases as the amount of water increases, although not significantly. The final ammonia levels are approximately proportional to the initial amounts of water in the system. The calculations have shown that a relatively small amount of oxygen in the system will suppress ammonia production completely [Henshaw et al.]. Therefore, for in principle the same reasons as for radiolytic production of nitric acid, internal stress corrosion

cracking due to ammonia production can be dismissed as a failure mode also for the outer copper shell [Marsh, Henshaw et al.].

4.2 Processes outside canister

The copper canister corrosion scenario is very similar to the KBS-3 scenario at least up to canister failure. Therefore, the KBS-3 analysis has been adopted also for the analysis of the Advanced Cold Process Canister. The possibilities for refining or making a more "realistic" analysis of the progress of copper corrosion have not been addressed since they are not considered as unique features for the advanced canister.

4.2.1 Mechanical actions

4.2.1.1 Strains caused by shrinking during the cooling period

In the present design there is a gap of 1 mm between the inner steel canister and the outer copper canister at room temperature. At maximum service temperature, this gap will increase with about 20% [Salo & Raiko]. The gap is expected to be closed by creep deformation of the copper. If this creep deformation takes place at the maximum temperature, the subsequent cooling would result in a tensile strain in the copper layer of less than 0.1 %. At corners and other geometric discontinuities the strain can be somewhat higher [Raiko].

4.2.1.2 The effect of corrosion product expansion on pressure loads

As defined in Section 4.2.2, the failure scenario is the penetration of a pit after a general corrosion in

the range of 1 to 2 cm. The build-up of corrosion products during general corrosion results in a volume increase by about 40%. This volume increase will compress the bentonite, resulting in an increase in pressure and a decrease in hydraulic conductivity. With a general corrosion corresponding to 2 cm copper, the compression of the bentonite will be about 2%. This corresponds to a pressure increase in the range of 5 to 10 MPa, depending on the density of the bentonite [Börgesson et al.]. A bentonite with density (water saturated) of 2.0 $g \cdot cm^{-2}$ will have a swelling pressure of less than 5 MPa and still retain the desired properties concerning hydraulic conductivity. Using a bentonite of this density the increase in swelling pressure due to corrosion would be low enough so that the total pressure will not exceed the canister design pressure of 15 MPa.

Local variation in corrosion must also be considered [Raiko]:

1) Variation in corrosion along the height of the canister will not cause additional problems as long as the corrosion is axi-symmetric. The maximum allowed pressure increase is still limited to the design pressure.
2) Angular variations in corrosion are potentially more severe, since they have a potential for lowering the stability margins of the canister by causing local flattening of the inner steel cylinder. However, the local deformation possibly caused by realistically anticipated uneven corrosion is expected to be moderate compared to the local flattening allowed in the standards. Not until the outer copper shell is completely corroded through, the local flattening will approach the maximum allowed local flattening. Furthermore, the pressure exerted by the corrosion products is a displacement controlled load. This means that the load does not follow the structure, if the structure is deflected.

Thus a corrosion product expansion pressure alone cannot collapse the steel canister as long as the global ovality of the steel cylinder is not exceeding the values allowed in the standards.

4.2.2 Copper canister corrosion

4.2.2.1 Copper canister corrosion before closure of repository

During this phase, the external copper surface will be contacted with nominally dry compacted bentonite assuming that the repository will be pumped and thus preventing its saturation. At the expected gamma-dose rates a low production rate of nitric acid through radiolysis of the moist air can be expected [Marsh]. However, in view of the calcite content of the bentonite, this very low rate of production of nitric oxide will be neutralized and will present no threat to the canisters [Wanner].

4.2.2.2 Copper canister corrosion after closure of repository

Since copper is thermodynamically stable in pure water, the corrosion of the canister will be controlled by the supply of corrodants from the environment. These are in the initial stage oxygen trapped in the tunnels and deposition holes and oxygen (hydrogen peroxide) produced by radiolysis of water. In the longer time perspective, oxygen may be transported to the canister through the groundwater. This is, however, more unlikely since the deep groundwaters are expected to be reducing, in which case the main corrodant will be sulphides. These sulphides may be supplied by the buffer mass in the deposition holes and the tunnel filling materials. The supply of sulphides from these sources is limited, but there may be a continuous supply from the groundwater,

which may contain sulphides at the level of about 0.5 $mg \cdot dm^{-3}$. A corrosion evaluation has been presented by the Swedish Corrosion Institute. There have been no developments that indicate that this evaluation should be revised at this stage except in details (see Section 4.2.2.4). Although the central scenario for KBS-3 was a low salinity water, analysis of the effect of chloride concentrations up to 35,000 ppm on the stability of copper was performed. It was found that also for this high salinity, the presented analysis was valid. Recently, a thermodynamic study has been performed for a water containing 3.0 M Cl^-. Also at these very high chloride concentrations, it was found that the effect on the copper corrosion was negligable [Taxén]. A brief summary of the KBS-3 analysis is given below.

4.2.2.3 Corrosion by oxygen

The oxygen available for corrosion is the oxygen initially present in the deposition holes and in the tunnels. The oxygen in the deposition holes is assumed to be consumed entirely by copper corrosion during the initial 1000 years. Of the oxygen in the tunnels, only a fraction will reach the canister during a time period of less than 10,000 years, while most of the oxygen will be consumed by other oxidation processes in the near-field. From a mass balance calculation, the total amount of corroded copper per canister can be calculated, see Table II.

Table II. Quantity of oxygen supplied to the canister surface, expressed in equivalent quantities of Cu(I) in kg.

Reactant	Exposure time, years			
	10^3	10^4	10^5	10^6
Initially in deposition hole	4.8	4.8	4.8	4.8
From tunnel	0.30	0.38	0.38	0.38

4.2.2.4 Corrosion by radiolysis products

For the purpose of this study, the analysis of the radiolysis from spent fuel disposed of in copper canisters presented in [Christensen & Bjergbakke 1982] is still valid. Although refinements can be made, they do not seem to be justified in view of the relative unimportance of radiolysis for the corrosion of the copper canisters.

At the radiation levels expected outside the canister, a maximum of 4.1 kg of copper can be corroded over 10^6 years.

Another finding in [Christensen & Bjergbakke 1982] is that at dose rates higher than $5 \cdot 10^{-2}$ rad$\cdot$s^{-1}, the hydrogen concentration in water is constant at about 1 mmol$\cdot$dm^{-3}. This is well below the solubility of hydrogen.

4.2.2.5 Corrosion by sulphides

As for oxygen, the sulphides can be supplied from the buffer mass/backfill in deposition holes and tunnels as well as from the groundwater. In addition to these sources, it can also be produced from sulphates through microbial activity. The resulting corrosion is presented

in Table III. The analysis has been made assuming that the bentonite will be subjected to oxidizing treatment to reduce the contents of sulphides and organic matter. For sulphides produced through microbial activity, it has been assumed that 5.6 mg of organic matter will give rise to 1 mg of sulphide and that organic matter in the groundwater will increase the sulphide concentration with 1 $mg \cdot dm^{-3}$. As was discussed in KBS-3, inorganic reduction of sulphate to sulphide is an extremely slow process and can, also for the time perspectives for a nuclear waste repository, be disregarded from.

Table III. Quantity of sulphide supplied to the canister surface, expressed in equivalent quantities of Cu(1) in kg.

Reactant	Exposure time, years			
	10^3	10^4	10^5	10^6
Initially in deposition hole with 0.02% S in bentonite	3.5	3.5	3.5	3.5
Formed through microbial activity in deposition hole	2.5	2.5	2.5	2.5
From tunnel:				
- with 0-0.02% S in bentonite	0.004	0.035	0.35	3.5
- formed through microbial activity	0.001	0.006	0.06	0.6
From groundwater via fractures	0.010	0.095	0.95	9.5
Formed through microbial activity in groundwater	0.010	0.095	0.95	9.5

4.2.2.6 Form of attack

As can be seen in Table IV, the corrosion attack that can occur on the copper canister will only be of importance if it has local character. From uniform attack only, the canister will not be penetrated until after over 70 million years. The most important form

of localized corrosion to be concerned with is pitting.

Table IV. Total attack on the canister as a function of exposure time.

Reactant	Depth (mm) of attack during following exposure time (years)			
	10^3	10^4	10^5	10^6
Supplied form the outside	0.12	0.12	0.18	0.68
Radiolysis oxidants	0.00	0.00	0.00	0.04
Average penetration	0.12	0.12	0.18	0.72
Max. pit depth (P_f=5)	0.6	0.6	0.9	3.6

The pitting attack on copper under the relevant conditions appears to give rise to pits with a relatively low aspect ratio (or pitting factor, P_f). As was discussed in KBS-3, a pitting factor of 2 to 5 is probably most realistic. In the analysis, a pitting factor of 5 has been assumed. This results in a calculated canister life-time of more than 10 million years as determined by failure through pit penetration of the copper shell (see data presented in Table IV).

The mechanisms behind pitting corrosion on copper under reducing conditions are not fully understood, but there is reason to assume that it will be even lower than presently assumed. Work on this has been in progress for some years within the SKB programme, but no conclusive data have so far been obtained. In view of the expected relatively low pitting factor, factors like local variations in the availability of sulphides may well be determining for the progress of the corrosion.

However, no data are available and since this is related to copper corrosion under repository conditions in general and not specifically to the advanced canister, such an analysis, if necessary, can be performed at a later stage as a refinement of the analysis.

4.2.2.7 Discussion on copper corrosion

The analysis presented above is based on the assumption that the bentonite used in the deposition holes will be heat treated in order to reduce its content of organic matter and sulphides. This bentonite is then rapidly (within 1,000 years) depleted in sulphides. Untreated bentonite may have a total sulphur content of up to 0.1 %. A total sulphur depletion, assuming that the pore water concentration of sulphides is constant at 1 mg/l, would require a time period of 350,000 years. The corresponding amount of copper corroded will be some 100 kg or a corrosion depth of less than 1 mm. During that period, there can be no sulphide contribution from the groundwater or tunnels, since the sulphide concentration in the pore water is equal to or exceeds that of the surrounding fluids [Sellin]. Thus, also with bentonite of much higher sulphur content, the canister will have an expected service life well of millions of years.

4.2.3 Chemical action on the bentonite

During the corrosion of copper under both oxidizing and reducing conditions, copper will dissolve. A modelling study of the copper - cation exchange processes in bentonite using available, conservative, data has shown that the copper ions released from the canister will have a negligible effect on the clay composition both

under oxidizing and reducing conditions due to the very low solubility of copper [Sellin].

The sulphide corrosion proceeds under hydrogen evolution. In the long term, the corrosion rate is extremely low and the hydrogen produced will easily escape through diffusion. The initial corrosion, caused by the sulphides and sulphates (reduced to sulphide through microbial activity) can conceivably result in a hydrogen production rate too high to allow escape through diffusion. However, adopting the analysis made by [Neretnieks] and assuming a pressure of 15 MPa (hydrostatic pressure plus bentonite swelling pressure) and a hydrogen diffusivity of $2 \cdot 10^{-11}$ $m^2 \cdot s^{-1}$, hydrogen corresponding to a copper corrosion rate of several micrometer per year can escape. The uncertainties in the calculation is estimated to be plus/minus a factor of five. The average corrosion rate during the first 1,000 years is about 0.12 $\mu m \cdot a^{-1}$ and based on this analysis, hydrogen will escape through diffusion and have no potential adverse effect on the bentonite. As was discussed in Section 4.2.2.4, a more recent analysis of the copper corrosion caused by sulphides present in the bentonite has shown that the assumption used in KBS-3 are overly conservative. The time period necessary to consume all sulphides is actually exceeding 10^5 years for a bentonite containing 0.2 % of sulphide [Sellin]. In view of this, a hydrogen production rate that will endanger the integrity of the bentonite can be excluded.

5 DEFINITION OF FAILURE SCENARIO

As has been discussed above, the service life of the canisters will well be several million years. At the time of failure, the radiotoxicity of the spent fuel originating from fission products and actinides will have dropped to the level of natural uranium. This is

illustrated in Figure 4. As can be seen, there are only a few nuclides that are of importance for the toxicity of the fuel after some thousand years. At the time of canister failure through general and pitting corrosion, the waste is not very different from the naturally occurring radionuclides in nature. Thus, the same type of precautions would be necessary to avoid excessive doses as would be needed for a naturally occurring high grade uranium deposit.

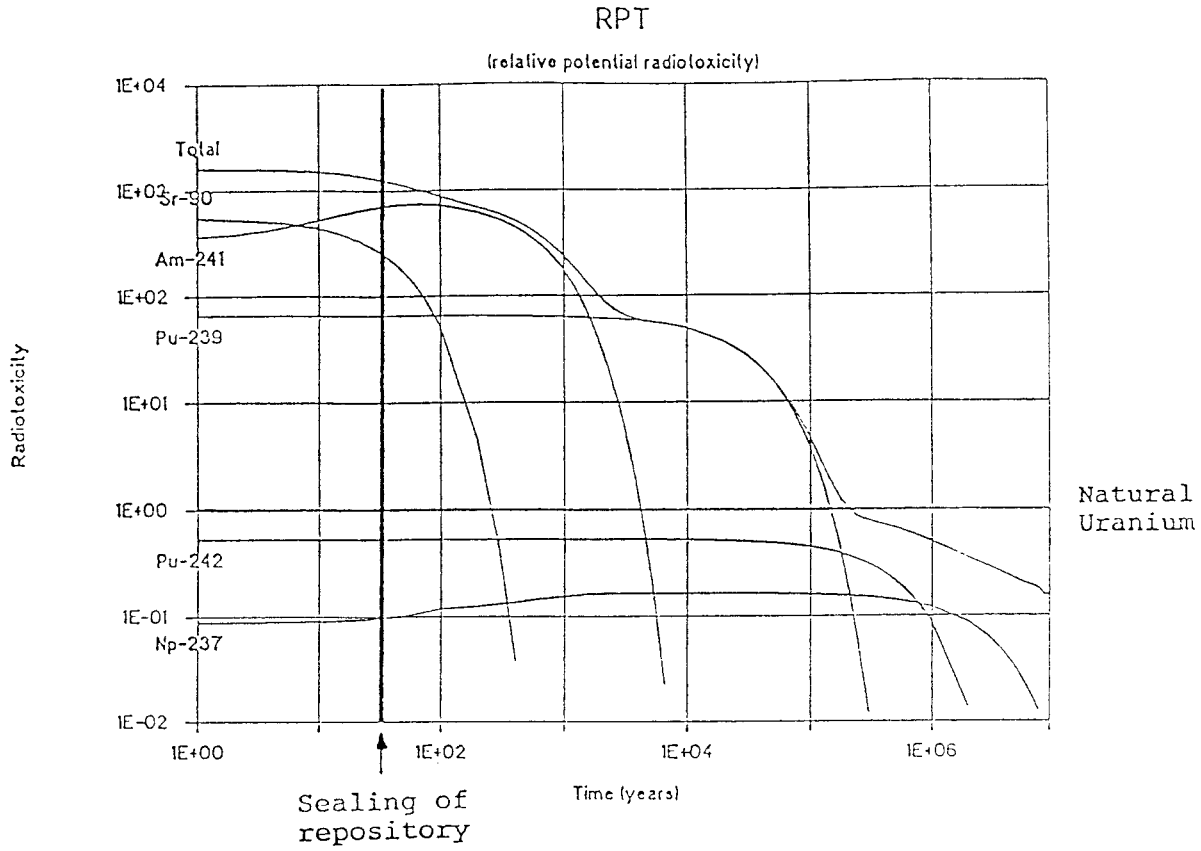

Figure 4: Relative potential radiotoxicity for the dominating nuclides as compared to the radiotoxicity of natural uranium.

In view of this, the highest need for analysis as well as for proven safety would be for scenarios which could cause release of radionuclides to the biosphere in the

period up to some several thousand years. Thus, there is little need to put a lot of effort in predicting the behaviour of the biosphere, or even the geosphere, after the next glaciation. In accordance with this, the analysis of post-failure behaviour has been focussed on low probability failures from faults in the canisters. The mechanisms which have been identified as having the potential to cause a breach over a time period shorter than one million years are:

(a) A defect in the closure weld of the copper canister.

(b) Internal stress corrosion cracking of the carbon steel vessel due to nitric acid production leading to mechanical failure of the complete canister (ie only feasible in the extreme case when the water volume sealed into a canister is substantially increased).

(c) Internal stress corrosion cracking of the outer copper shell due to ammonia production (ie again only feasible if appreciable quantities of water are sealed into a canister).

(d) Mechanical failure due to a large shear fracture of the host rock.

It should be emphasized that all four of these scenarios are improbable in the sense that the probability for occurring can be controlled to a large extent through quality control measures during the manufacture of the canisters, during loading the canisters and during the emplacement in the deposition holes in the repository. They are also likely to result in a relatively narrow fracture which may stretch all along the periphery of the canister but with a large percentage of the canister remaining intact and capable of functioning as a barrier to activity release. Nonetheless, for completeness, the

behaviour of the canister subsequent to penetration by one or other of these processes will be considered in Section 6.

6 PROCESSES AFTER CANISTER FAILURE

Many penetration scenarios resulting from the events listed above could be postulated depending on the failure mechanism. A defect in the closure weld will result in a fracture at the top of the canister. Stress corrosion cracking will more likely occur at the base of the canister, where the liquids will accumulate, while a shear fracture could take place anywhere between these two extremes. As base scenario for failure, a simplified generic case will be considered involving a circumferential crack penetrating the canister at the bottom. This is assumed to occur after saturation of the repository and the hydrostatic head of ca 5 Mpa will drive water through the breach into the canister. Such a scenario can be considered as conservative in the respect that a maximum quantity of contaminated water, which has penetrated the canister, will be pushed out as a result of hydrogen pressure build-up inside the canister.

Depending on the width of the crack, it may be pure water, or if the crack is wide enough (ca 1 mm), water saturated bentonite will also intrude. However, if the canister is filled with a granular material with a particle size of less than ca 1 mm, the intrusion of bentonite will be stopped by the filling material and, thus, at the most fill the crack. An analysis of the effects of bentonite intrusion into the canister has been performed [Börgesson 1990b]. The worst case is when the bentonite is allowed to fill, without resistance, a canister which does not contain any particulate material. This will result in a loss of buffer bentonite corresponding to a drop in density locally outside the

canister to, conservatively, about 1,800 $kg \cdot m^{-3}$, neglecting the relaxation of the pressure build-up caused by the copper corrosion products. Also at this density, the clay barrier is still effective [Börgesson 1990b]. This density decrease is associated with an increase in hydraulic conductivity of no more than about one order of magnitude [Börgesson et al.].

6.1 Corrosion of the interior of the steel canister

The intrusion water or water saturated bentonite into the canister will result in corrosion of the internal canister walls. The interior of the canister is expected to be oxygen free, or as a result of corrosion, rapidly become oxygen free. As a consequence, the corrosion will result in the production of hydrogen. The results of experimental studies of the anaerobic corrosion of carbon steel at temperatures relevant to repository conditions have recently been reviewed in a preliminary assessment of the corrosion behaviour of the Advanced Cold Process Canister [Marsh]. It was found that there is a relatively wide spread in the reported data. At temperatures below 50°C, the typical corrosion rate appears to be in the range of 0.2 to 6.5 $\mu m \cdot a^{-1}$. This corrosion has a potential for occurring both on the interior steel surface and in the narrow gap between the steel canister and the outer copper shield. Based on this review, the corrosion rate of 6.5 $\mu m \cdot a^{-1}$ was chosen in order to ensure some conservatism in the corrosion evaluation.

The hydrogen associated with these corrosion rates will not be able to escape by diffusion through the relatively narrow breach in the canister. Thus, a scenario involving gaseous hydrogen must be considered.

Another issue which needs to be addressed is the possible influence of copper on the corrosion rate of the carbon steel. Conceivably, the presence of a copper surface area comparable to the steel surface area could accelerate the corrosion, since the cathodic, water reduction reaction could take place also on the copper surface, assuming that the cathodic reaction is rate limiting for the corrosion. This may not necessarily be the case, although it is conservative to assume so.

Copper and iron have very similar cathodic reaction properties and it would be expected that the coupling of roughly equal areas of the two metals would lead to a doubling of the iron corrosion rate in the narrow gap between the copper and the steel vessels [Marsh]. For the interior steel surface, as well as for the influence of the outer copper surface, the situation is more difficult to assess. It depends on factors such as the electrical conductivity of the groundwater or water saturated bentonite and the width and geometry of the breach in the canister [Marsh]. However, the effect will be much smaller than for the case discussed above. If the current is evenly distributed over the steel surface it will only produce an additional corrosion rate of about 0.1 $\mu m \cdot a^{-1}$. This is small in comparison to the rates quoted above, and consequently the effect of the external copper surface can be neglected [Marsh].

6.2 Escape of hydrogen gas

The corrosion rate of 1 $\mu m \cdot a^{-1}$ is equivalent to a hydrogen production rate of about 3.1 $dm^3 \cdot m^{-2} \cdot a^{-1}$. This hydrogen evolution will start as soon as the intrusion of water starts. The actual scenario depends on the location of the breach in the canister along its axis. Generally, in an initial stage hydrogen production and

water intrusion will occur simultaneously. This will proceed until the hydrogen pressure is equal to the hydrostatic pressure outside the canister. Once the hydrostatic pressure is exceeded, additional hydrogen pressure build-up will result in an outflow of water from the canister.

The situation for a circumferential breach at the bottom of the canister is illustrated in Figure 5 for a bentonite density of 2,000 $kg \cdot m^{-3}$ and a hydraulic conductivity of 10^{-13} $m \cdot s^{-1}$. The corrosion rate is assumed to be 1 $\mu m \cdot a^{-1}$. Water inflow occurs for about 300 years at which time the canister is filled to about 75 %. After this, the additional hydrogen pressure build-up results in an outflow of water and the canister is empty after some 1500 years [Börgesson 1990a]. At other positions of the breach, only the amount of water above the breach will be pushed out.

For comparison, Figure 6 shows the same scenario for a corrosion rate of 10 $\mu m \cdot a^{-1}$. As can be seen, the water inflow period is now limited to about 150 years at which time only a few percent of the canister is filled with water. The outflow period is also about 150 years [Börgesson 1990a]. The average outflow rates are 0.2 and $2 \cdot 10^{-4}$ $dm^3 \cdot a^{-1}$, respectively, for the two scenarios.

After the transient period discussed above the corrosion will proceed at about the same rate as discussed above if there are substantial quantities of water remaining in the canister until all the water is consumed by corrosion reactions.

The equilibrium hydrogen pressure for anaerobic corrosion of iron is in the range of 5 to 90 MPa depending on temperature and corrosion reaction. It is unlikely that such high internal pressures will be reached before the gas escapes through the bentonite as gas bubbles.

However, in the analysis of the Swiss repository concept, Nagra [Project Gewähr] addressed a very similar problem and the conclusion was that at increasing gas pressures, a non-linearity in the gas permeability occurs which can be explained by "channelling effects" or "percolation effects", whereby the gas can escape through a system of connecting pores. These pores only represent a very small fraction of the total pore water volume in the bentonite (ca 1.7 m^3) and according to available data, this process is reversible so that a decrease in gas pressure is followed by a decrease in permeability. Through this process sufficient quantities of hydrogen could escape so that no unacceptably high pressure is expected to build up either in the vicinity of the canister or in the surrounding rock [Pusch et al., Pusch].

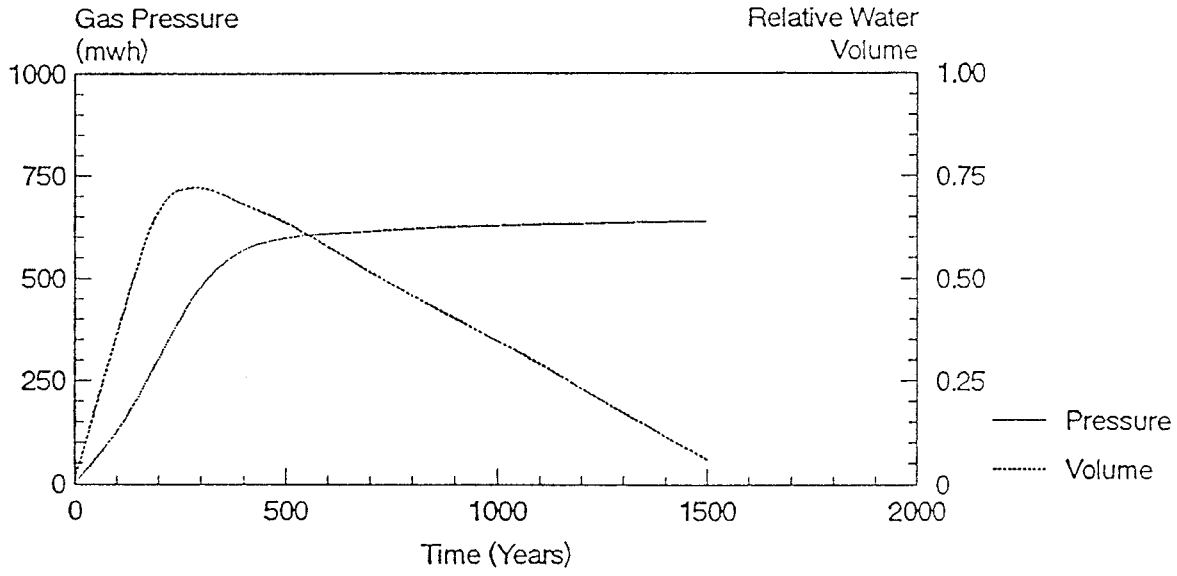

Figure 5: Hydrogen pressure build-up and volume of intruded water as a function of time after canister failure through a narrow circumferential crack at the canister bottom for a corrosion rate of 1 $\mu m \cdot a^{-1}$.

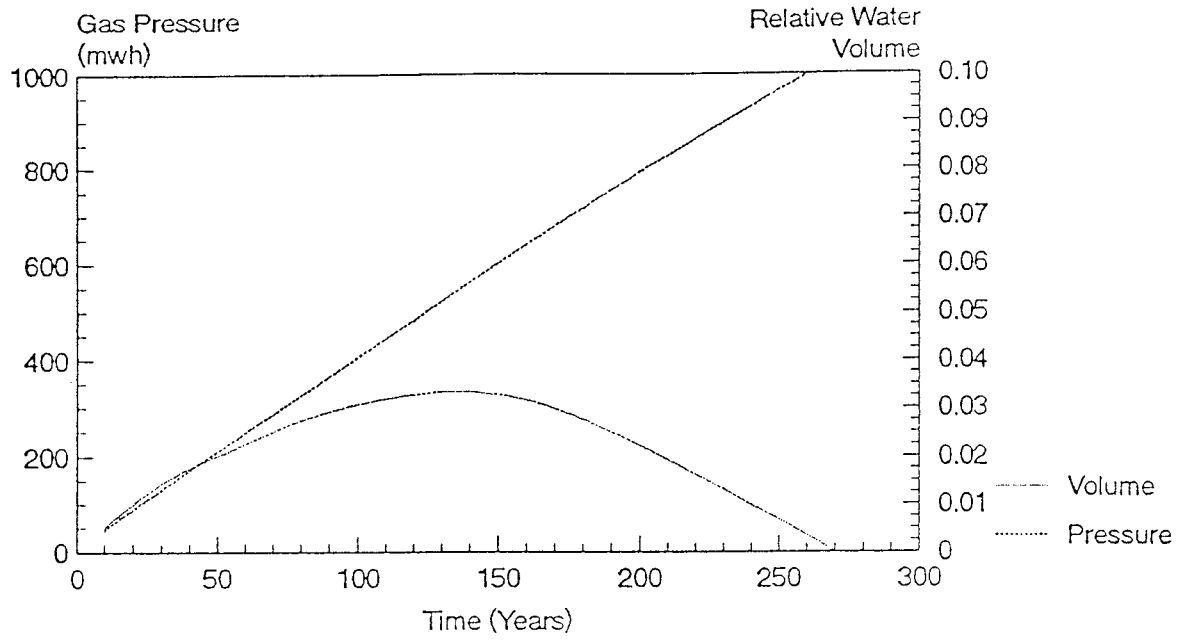

Figure 6: Same as Figure 5, but for a corrosion rate of 10 $\mu m \cdot a^{-1}$.

6.3 Modelling canister corrosion

In the preliminary assessment made by Marsh, several simplifying assumption had to be made when the evolution of hydrogen as a function of time was calculated. Some of these assumptions concerned the water ingress scenario and the geometry of the canister. Three scenarios were analysed, involving different locations of the canister penetration. These analyses showed that depending on the crack location, the hydrogen release rates range between 2 and 6 $dm^3 \cdot a^{-1}$ (at 10 MPa), and may persist for 7,000 - 11,000 years. However, the scenarios chosen may not have bracketed the full range of behaviour of the system. Several unrealistic assumptions, such as immediate flooding of the canister after breach, were also made in order to simplify the analysis. Therefore, a further assessment study was performed of the areas where the preliminary study had identified the need for

a more quantitative evaluation. This study involved modelling in much greater detail of the water ingress into the canister and of the canister geometry. Two basic scenarios were analysed, assumed to bracket the two extreme cases; the case with the highest hydrogen production rate and the case with the longest hydrogen production period [Henshaw et al.]. For these two scenarios, sensitivity tests have been performed where the effects of variations in key parameters such as corrosion rate, galvanic contact, crack width and accumulation of corrosion products have been studied. The base case parameters are given in Table V.

Table V. Base case parameters for the Advanced Cold Process Canister corrosion performance calculation

Corrosion rate	6.5 μm/year
Galvanic enhancement	none
Crack width	1 mm

The two base cases are:

(a) crack in copper canister at base, crack in steel canister at top.

For this case, the corrosion behaviour can be divided into two periods: Period 1, when water enters the canister until the hydrogen gas pressure equals the external pressure and flow reverses. The remaining water inside the canister is then consumed by corrosion reactions. Period 2, when the corrosion in the gap between the copper and steel canisters occurs by diffusion of water vapour through the crack in the outer canister,

and corrosion product precipitates. This corrosion will then cease when the annulus fills. The hydrogen production rate for this scenario is illustrated in Figure 7. Comparison with the preliminary assessment shows the hydrogen release rates were over-estimated by assuming the the canisters filled with water immediately. In that case, a total of 29,000 dm^3 of hydrogen was produced, while the more realistic analysis gave 590 dm^3.

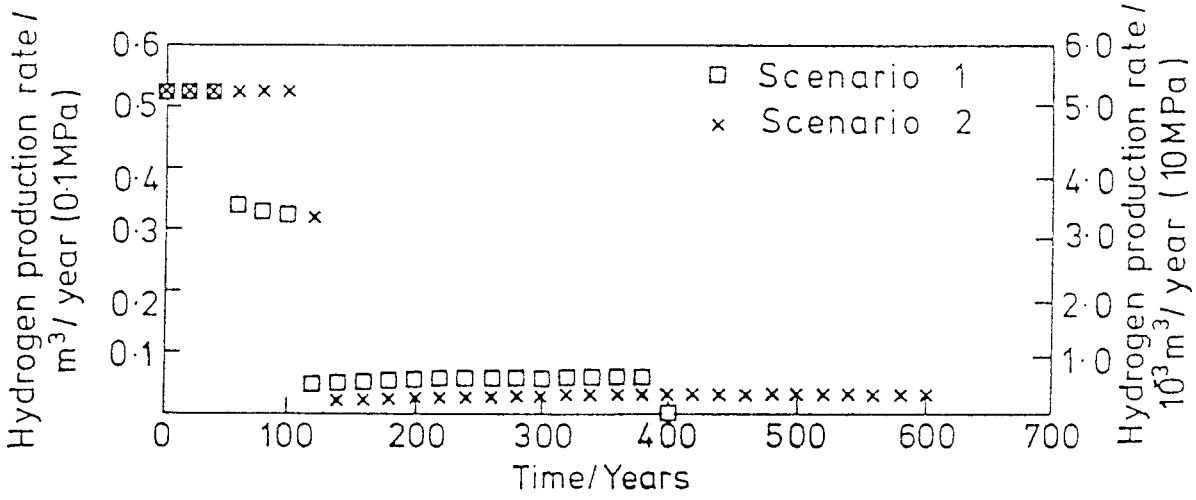

Figure 7: Predicted hydrogen production rates for canister failure cases 1 and 2.

(b) Case 2: Crack in outer canister at the top, crack in inner canister at top.

Also in this case, the corrosion behaviour can be divided into two periods: Period 1, when water enters the canister until the hydrogen gas pressure equals the external pressure and flow reverses. The remaining water inside the canister is then

consumed by corrosion reactions. Period 2, when corrosion in the annulus between the copper and steel canisters and the corrosion inside the steel canister is controlled by diffusion of water vapour through the crack in the canisters. In this case, the total amount of hydrogen produced is the same as was found in the preliminary analysis. However, the production rates are lower and, hence, the period during which hydrogen is produced, longer (ca 50,000 years compared to ca 10,000 years). The hydrogen production rates for the first several hundred years are shown in Figure 7 and compared with the predictions from Case 1.

Table VI. Summary of hydrogen production rates at 10 MPa ($m^3.a^{-1}$/number of years) as a function of variations in the base parameters

	Base Case	Corrosion Rate 1 mic/yr	Galvanic Contact	Crack Width 2mm	Decreasing Current 1/thickness	Preliminary Assessment
Case 1)	$5x10^{-3}$/60y $3.5x10^{-3}$/40y $5x10^{-4}$/300y	$8x10^{-4}$/4000y $4x10^{-4}$/2000y	$8x10^{-3}$/20y $7x10^{-3}$/20y $6x10^{-4}$/280y	$5x10^{-3}$/60y $4x10^{-3}$/40y $1x10^{-3}$/300y	$3x10^{-3}$/40y $1x10^{-3}$/1200y $2x10^{-5}$/>60000y	$6x10^{-3}$/6y $4x10^{-3}$/7200y
Total gas/ m^3	0.59	4	0.46	0.76	>2.5	29
Time years	400	6000	320	400	>60000	7200
Case 2)	$5x10^{-3}$/120y $3x10^{-4}$/$5x10^4$y	$8x10^{-4}$/2000y $3x10^{-4}$/$5x10^4$y	$8x10^{-3}$/20y $4x10^{-3}$/80y $3x10^{-4}$/$5x10^4$y	$5x10^{-3}$/100y $6x10^{-4}$/$2.5x10^4$y	$3x10^{-3}$/120y $1x10^{-3}$/1200 y $4x10^{-5}$/>60000	$6x10^{-3}$/180y $2x10^{-3}$/7000y
Total gas/ m^3	15	15	15	15	15	15
Time/ years	$5x10^4$	$5x10^4$	$5x10^4$	$2.4x10^4$	>60000	7200

The results of the variation analysis are presented in Table VI. As can be seen, the maximum hydrogen production occurs when the annulus is full of water (maximizing the galvanic effect) and there is some water in the inner canister. The results are most sensitive to the effect of a decreasing corrosion current with time. This effect has been investigated with the model assuming that the corrosion rate decreases inversely with the thickness of the corrosion product layer. In this scenario, the short term hydrogen production rates are lower, but the production continues over very much extended corrosion periods. However, there are at present very little data on the variation of the corrosion rate with time (i e with the growth of corrosion products).

6.4 UO_2 fuel dissolution

Once the fuel has been exposed to the solution, basically one of two modes of dissolution can occur.

a) The immediate near-field conditions are such that UO_2 or U_4O_9 is stable.

b) UO_2 is not thermodynamically stable, but oxidizes to form a more oxygen-rich uranium oxide, such as U_3O_8 or UO_3 or other U(VI) solids.

In case a), the mobilization of most fission products and actinides will be controlled by the solubility of the UO_2 solid. The release, however, of sparingly soluble radionuclides will depend on their solubilities. This will be the case under reducing conditions. At higher redox potential, case b) will be valid in which case the mobilization of most fission products and actinides will be controlled by the rate of transforma-

tion of UO_2 to higher oxides. Also in the case, the release of sparingly soluble radionuclides will depend on their solubilities.

The conditions inside the steel canisters will be complex due to progressing steel corrosion and alpha-radiolysis of the intruding water. In the analysis of the WP-Cave concept, Christensen and Bjergbakke [1987] showed that if Fe^{2+} is readily accessible, radiolysis will produce H_2 and Fe(III) thus maintaining a reducing environment inside the canisters. Furthermore, calculations performed by AECL [Tait & Johnson], have shown that a relatively low concentration of hydrogen in the water would suppress the formation of oxidant through alpha-radiolysis. The Canadian study also supported the conclusion reached by Christensen and Bjergbakke that when Fe^{2+} is present in the solution, reducing potentials are maintained. These observations point in the direction of applying a model for spent fuel dissolution under reducing conditions, ie the case a) above.

However, alpha-radiolysis only affects a very thin water layer close to the fuel surface and the oxidants may react with the UO_2 before encountering Fe^{2+} ions. The result of this may be a radiolysis controlled oxidative dissolution at the fuel surface followed by a re-precipitation of the redox sensitive elements already inside the canister, since the bulk conditions will be reducing due to the presence of Fe(II) corrosion products. This corresponds to oxidative dissolution as described in case b) above, but followed by precipitation at a static redox front in the immediate vicinity of the spent fuel.

Although it seems reasonable to assume that the fuel dissolution will occur under reducing conditions for the hydrogen pressures foreseen inside the canister, it may be prudent to also discuss, for comparison, the

consequences of a radiolytically controlled oxidative dissolution. In the former case, the same solubility/mass transport controlled dissolution model used in KBS-3 is applicable, with the modification that uranium and radionuclide solubilities valid for reducing conditions are used. For the latter case, a simplified model for radiolytically controlled dissolution/precipitation is currently being developed [Werme et al.] and can be applied for a preliminary assessment.

6.5 Release of radionuclides

6.5.1 Dissolution under reducing conditions.

The dissolution of the fuel is assumed to take place at a redox potential of -530 mV as controlled by the hydrogen present in the system. Outside the canister, the nominal redox potential of deep groundwaters at -200 mV is maintained. No transport restriction imposed by the narrow breach in the canister wall has been taken into account. A possible early pulse release due to the "push-out" of water during the transient phase is dealt with in section 6.5.3. The solubility limits used for the different elements are those of the EQ3/6 code, where amorphous plutonium- and neptuniumdioxide have been assumed.

The results of the calculation are shown in Figure 8 for one canister failing after 1,000 years. All data refer to release from the buffer mass into the host rock. No transport restrictions caused by the canister and the canister corrosion products have been taken into account. As can be seen, the releases of radionuclides are very low, less than one becquerel per canister and year for all elements of interest. Thus, there is little need for any detailed modelling of the near-field. However, after all steel has been consumed

by corrosion (ca 50,000 years), the trapped hydrogen will escape through diffusion over a period of some thousand years and the subsequent fuel dissolution will be controlled by radiolytically produced oxidants, see section 6.5.2.

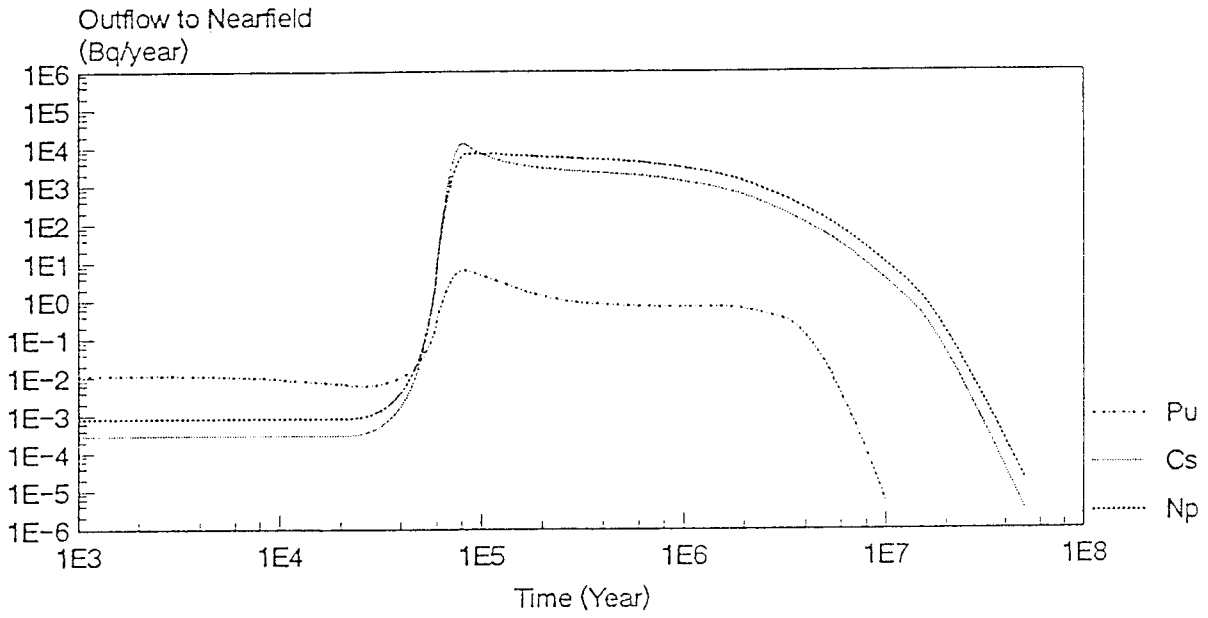

Figure 8: Release from the near-field in $Bq \cdot a^{-1}$ from one canister assuming reducing conditions, controlled by the hydrogen over-pressure, to prevail inside the canister.

6.5.2 Radiolytically controlled dissolution

In this model, it has been assumed that reducing conditions prevail in the near-field. The only possible supply of oxidants is the alpha-radiolysis. Due to the very short range of the alpha-particles, local oxidizing

conditions prevail at the fuel surface, leading to an oxidative dissolution of the fuel matrix followed by an immediate re-precipitation of the redox sensitive elements. The actual contribution from radiolysis to the dissolution rate is not yet well known. In the presented example (Figure 9) empirical data for the fuel dissolution rate have been used assuming that the strontium release rate is an indicator of the rate of UO_2 alteration. A more detailed description of the release model is given in [Werme et al.]. Conservatively, the observed release rates for strontium in an aerated system has been used. The results for the releases of neptunium, cesium and plutonium from the fuel in one canister for a failure time of 1,000 years are presented in Figure 9. Cesium is not redox sensitive and will be released at the fuel alteration rate as controlled by the radiolysis rate. For neptunium and plutonium, the release rates will be controlled by their respective solubilities. The redox potential in the near-field has been assumed to be the same as in the far-field, ie ca -200 mV. The release rates are in the same range as the ones used in KBS-3.

For comparison, Figure 10 shows the same model applied to a situation where the fuel alteration rate is a factor of ten lower. This is what is measured in laboratory experiments when hydrogen gas, in the presence of a palladium catalyst, has been added to the solution as well as to the atmosphere. This is the closest laboratory simulation that has been performed of the conditions inside the canister. In the experiments, only about 6 kPa partial pressure of hydrogen was use

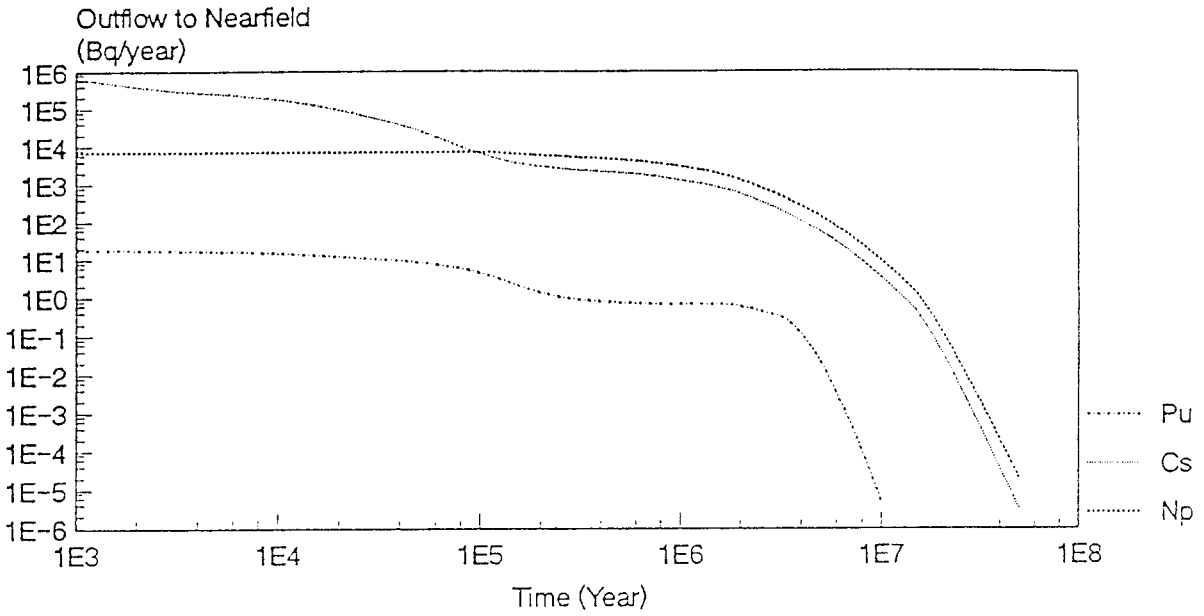

Figure 9: Release from the fuel for a scenario where the to fuel dissolution is controlled by the alpha-radiolysis. A fuel dissolution rate as determined in laboratory experiments with free access to air is used. Reducing conditions are assumed to prevail inside the canister.

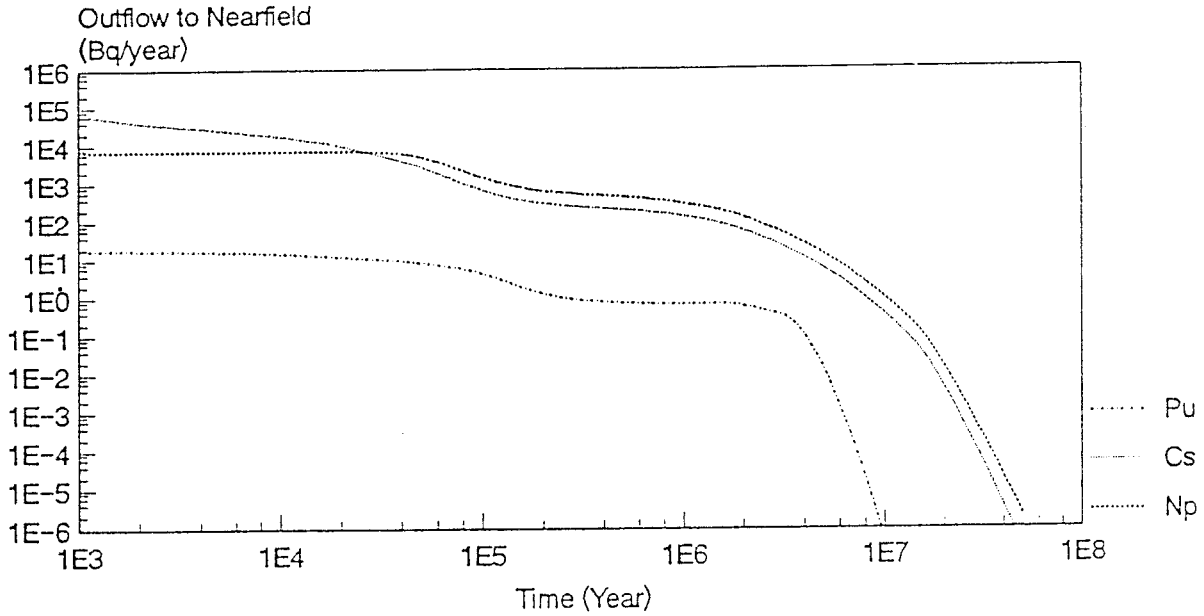

Figure 10: Same as for Figure 9, but fuel dissolution data obtained in the laboratory with hydrogen (and a palladium catalyst) present is used.

as compared to the partial pressure of 10 to 15 MPa foreseen in the laboratory. It is interesting to note that in this case the release of neptunium very rapidly becomes controlled by the fuel alteration rate rather than by the solubility of neptunium. The release of cesium is lowered in accordance with the lower fuel dissolution rate. For plutonium. there is no difference between the two cases since plutonium being controlled by its solubility in both cases.

In the model, no account has been taken for the additional constraints to release from the canister imposed by the transport through a narrow crack in the canister wall.

6.5.3 Instant release fraction

A certain fraction of volatile fission products such as cesium and iodine will be available for instant release. The size of the instant release fraction will depend on the in-reactor operation conditions, such as burnup and linear power rating. A typical value for this fraction is for current fuel 1 % of the total inventory, although it exceed even 10 % for some fuel rods. In the KBS-3 analysis [Bengtsson, KBS-3] an instant release to the pore volume (1.7 m^3) of bentonite buffer was assumed. The release from the buffer was spread in time due to the finite rate of displacement of the water volume containing the dissolved material. Conservatively, the same instant release can be assumed for the Advanced Cold Process Canister, although the present analysis indicates that the release to the bentonite buffer is more likely to take place over a period of up to 1,500 years, depending on the steel corrosion rate. For an instant release fraction of 10 %, KBS-3 gave release rates of $3.0 \cdot 10^5$ (Bq/canister, year) for iodine and $3.2 \cdot 10^6$ (Bq/canister, year) for cesium. The distribution

of canister penetrations in time will lead to an equilization of the release of iodine and cesium from the entire repository [KBS-3].

7 DISCUSSION

The present report is a preliminary analysis of the Advanced Cold Process Canister. It has been found that the expected service life of this canister with respect the general corrosion and pitting is, as expected, comparable to that of the KBS-3 canister. New data on the corrosion caused by sulphides present in the bentonite indicate that the KBS-3 analysis in some respects was over-conservative. Furthermore, in the safety analysis of KBS-3, full account was not taken for the expected service life of the canister. This has been done in the present analysis and, as result, the interest has been focussed of failure mechanisms other that general (and pitting) corrosion. These mechanisms are also associated with the specific design of the Advanced Cold Process Canister and, therefore, analysed in more detail.

The major differences are the processes associated with the fact that the Advanced Cold Process Canister has a void volume inside and that the iron is an important component in the canister. This requires the discussion also mainly two phenomena: the possible corrosion of the interior of the canister prior to penetration and the hydrogen producing corrosion of the iron components after penetration.

The corrosion of the interior of the canister was found to negligeable except, possibly, in the unlikely event when substantial quantities of water are carried over into the canister. Proper drying procedures and control measures will ensure that this will not be the case.

Two major, potential, consequences of the hydrogen production have been identified. It has been found that the hydrogen gas generated cannot escape through diffusion. A most probable scenario a scenario where gaseous hydrogen is released must be considered. The analysis indicates that this should not be detrimental for the overall performance of the waste package after failure of the canister.

One important potential advantage with the hydrogen gas evolution scenario has been identified. The presence of corroding iron and iron corrosion products will have a strong influence on the redox conditions thereby maintaining a stationary redox front inside the canister. The releases from the near-field under these conditions need to be analysed further.

At high partial pressures, it is even possible that the hydrogen gas will control the redox conditions. If this effect also overcomes the effects of radiolysis, which is the only source of oxidants inside the canister, it will have a dramatic effect on the releases from the fuel by stabilizing the UO_2 matrix and limit the releases to negligible levels for the first 50,000 years after an early failure. This scenario should be investigated further.

8 CONCLUSION

The analysis has shown that under foreseen operating conditions, internal processes cannot cause the canister breach, e.g. localized corrosion for the steel or copper canister can be dismissed as a failure mechanism.

The evaluation of the effects of processes outside the canister indicate that there is no rapid mechanism to

endanger the integrity of the canister. Consequently the service life of the canister will be several million years. This factor will ensure the safety of the concept.

For completeness also evaluation of post-failure behaviour was carried out. Analyses were focussed on low probability failures from faults in canisters.

Some items were identified where further research is justified in order to increase knowledge of the phenomena and thus strengthen the confidence of safety margins. However, it can be concluded that the risks of these scenarios can be judged to be acceptable. This is due to the fact that firstly, the probability of occurrence of most of these scenarios can be controlled to a large extent through technical measures. Secondly, these analyses indicated that the consequences would not be severe.

As a summary, according to this evaluation the Advanced Cold Process Canister seems to meet at least the same safety targets as the KBS-3 canister.

9 REFERENCES

A. Bengtsson, M. Magnusson, I. Neretnieks and A. Rasmuson 1983
"Model calculations of the migration of radionuclides from a repository for spent nuclear fuel" SKBF/KBS Technical Report 83-48.

L. Börgesson, H. Hökmark and O. Karnland 1988
"Rheology properties of sodium smectite clay" SKB Technical Report 88-30.

L. Börgesson 1990a
"Some aspects of the water intrusion scenario for the Advanced Cold Process Canister" SKB Work Report AR 90-12.

L. Börgesson 1990b
"Scenario of SKB/TVO-canister with special respect to the effect of bentonite intrusion into the canister" SKB Work Report AR 90-31.

H. Christensen and E. Bjergbakke 1982
"Radiolysis of groundwater from HLW stored in copper canisters", SKBF/KBS Technical Report 82-02.

H. Christensen and E. Bjergbakke 1987
"Radiolysis of ground water from spent fuel, stored according to the WP-Cave concept", SKB Work Report 87-21.

J. Henshaw, A. Hoch and S.M. Sharland 1990
"Further assessment studies of the Advanced Cold Process Canister", Harwell Report No. AEA D&R 0060.

KBS-3 1983
Final Storage of Spent Nuclear Fuel - KBS-3
SKBF/KBS

G.P. Marsh 1990
"A preliminary assessment of the Advanced Cold Process Canister", Harwell Report No. AEA INTEC 0011.

I. Neretnieks 1985
"Some aspects of the use of iron canisters in deep lying repositories for nuclear waste" Nagra Technical Report 85-35.

PROJECT GEWÄHR 1985
Nuclear waste management in Switzerland: Feasibility studies and safety analyses
Project Report NGB 85-09.

R. Pusch, L. Ranhagen and K. Nilsson 1985
"Gas migration through MX-80 bentonite", Nagra Technical Report 85-36.

R. Pusch, 1990
"Behavior of hydrogen gas in deposition holes and its dissipation through confining rock - application to the KBS-3 repository design", SKB Work Report AR 90-25.

H. Raiko 1990
"Some comment on the copper/steel canister design loads", VTT/YDI Technical report No YDI0028-1/90.

J-P. Salo and H. Raiko 1989
"The copper/steel canister design for nuclear waste disposal", TVO/KPA Technical Report 89-14.

A. Sanderson, T.F. Szluha and I A Macdonald 1989
"Assessment of nuclear waste disposal canister design", SKB Work Report AR 90-13

P. Sellin
"Modelling of copper ion/bentonite interaction" SKB Work Report AR 90-14

The Swedish Corrosion Research Institute and its reference group 1983
"Corrosion resistance of a copper canister for spent nuclear fuel", SKBF/KBS Technical Report 83-24.

J.C. Tait and L.H. Johnson 1986
"Computer modelling of alpha-radiolysis of aqueous solutions in contact with used UO_2 fuel" Proceedings of 2nd International Conference on Radioactive Waste Management, Canadian Nuclear Society, p. 611.

C. Taxén 1990
"Corrosion on copper in chloride containing waters. A thermodynamic study" SKB Work Report AR 90-29.

Transnucléaire 1989
Dossier de sûreté, Emballage TN 17/2
Rapport no 6117 - Z rev. 0.

H. Wanner 1986
"Modelling interaction of deep groundwaters with bentonite and radionuclide speciation" Nagra Technical Report 86-21.

L.O. Werme. P. Sellin and R.S. Forsyth 1990
"Radiolytically induced oxidative dissolution of spent nuclear fuel" SKB Technical Report 90-08.

List of SKB reports

Annual Reports

1977–78
TR 121
KBS Technical Reports 1 – 120.
Summaries. Stockholm, May 1979.

1979
TR 79–28
The KBS Annual Report 1979.
KBS Technical Reports 79-01 – 79-27.
Summaries. Stockholm, March 1980.

1980
TR 80–26
The KBS Annual Report 1980.
KBS Technical Reports 80-01 – 80-25.
Summaries. Stockholm, March 1981.

1981
TR 81–17
The KBS Annual Report 1981.
KBS Technical Reports 81-01 – 81-16.
Summaries. Stockholm, April 1982.

1982
TR 82–28
The KBS Annual Report 1982.
KBS Technical Reports 82-01 – 82-27.
Summaries. Stockholm, July 1983.

1983
TR 83–77
The KBS Annual Report 1983.
KBS Technical Reports 83-01 – 83-76
Summaries. Stockholm, June 1984.

1984
TR 85–01
Annual Research and Development Report 1984
Including Summaries of Technical Reports Issued during 1984. (Technical Reports 84-01–84-19)
Stockholm June 1985.

1985
TR 85-20
Annual Research and Development Report 1985
Including Summaries of Technical Reports Issued during 1985. (Technical Reports 85-01-85-19)
Stockholm May 1986.

1986
TR 86-31
SKB Annual Report 1986
Including Summaries of Technical Reports Issued during 1986
Stockholm, May 1987

1987
TR 87-33
SKB Annual Report 1987
Including Summaries of Technical Reports Issued during 1987
Stockholm, May 1988

1988
TR 88-32
SKB Annual Report 1988
Including Summaries of Technical Reports Issued during 1988
Stockholm, May 1989

Technical Reports

List of SKB Technical Reports 1990

TR 90-01
FARF31 –
A far field radionuclide migration code for use with the PROPER package
Sven Norman[1], Nils Kjellbert[2]
[1] Starprog AB
[2] SKB AB
January 1990

TR 90-02
Source terms, isolation and radiological consequences of carbon-14 waste in the Swedish SFR repository
Rolf Hesböl, Ignasi Puigdomenech, Sverker Evans
Studsvik Nuclear
January 1990

TR 90-03
Uncertainties in repository performance from spatial variability of hydraulic conductivities –
Statistical estimation and stochastic simulation using PROPER
Lars Lovius[1], Sven Norman[1], Nils Kjellbert[2]
[1] Starprog AB
[2] SKB AB
February 1990

TR 90-04
Examination of the surface deposit on an irradiated PWR fuel specimen subjected to corrosion in deionized water
R.S. Forsyth, U-B. Eklund, O. Mattsson, D. Schrire
Studsvik Nuclear
March 1990

TR 90-05
Potential effects of bacteria on radionuclide transport from a Swedish high level nuclear waste repository
Karsten Pedersen
University of Gothenburg, Department of General and Marine Microbiology, Gothenburg
January 1990

TR 90-06
Transport of actinides and Tc through a bentonite backfill containing small quantities of iron, copper or minerals in inert atmosphere
Yngve Albinsson, Birgit Sätmark, Ingemar Engkvist, W. Johansson
Department of Nuclear Chemistry, Chalmers University of Technology, Gothenburg
April 1990

TR 90-07
Examination of reaction products on the surface of UO_2 fuel exposed to reactor coolant water during power operation
R S Forsyth, T J Jonsson, O Mattsson
Studsvik Nuclear
March 1990

TR 90-08
Radiolytically induced oxidative dissolution of spent nuclear fuel
Lars Werme[1], Patrik Sellin[1], Roy Forsyth[2]
[1] Swedish Nuclear Fuel and waste Management Co (SKB)
[2] Studsvik Nuclear
May 1990

TR 90-09
Individual radiation doses from unit releases of long lived radionuclides
Ulla Bergström, Sture Nordlinder
Studsvik Nuclear
April 1990

TR 90-10
Outline of regional geology, mineralogy and geochemistry, Poços de Caldas, Minas Gerais, Brazil
H D Schorscher[1], M E Shea[2]
[1] University of Sao Paulo
[2] Battelle, Chicago
December 1990

TR 90-11
Mineralogy, petrology and geochemistry of the Poços de Caldas analogue study sites, Minas Gerais, Brazil. I: Osamu Utsumi uranium mine
N Waber[1], H D Schorscher[2], A B MacKenzie[3], T Peters[1]
[1] University of Bern
[2] University of Sao Paulo
[3] Scottish Universities Research & Reactor Centre (SURRC), Glasgow
December 1990

TR 90-12
Mineralogy, petrology and geochemistry of the Poços de Caldas analogue study sites, Minas Gerais, Brazil. II: Morro do Ferro
N Waber
University of Bern
December 1990

TR 90-13
Isotopic geochemical characterisation of selected nepheline syenites and phonolites from the Poços de Caldas alkaline complex, Minas Gerais, Brazil
M E Shea
Battelle, Chicago
December 1990

TR 90-14
Geomorphological and hydrogeological features of the Poços de Caldas caldera, and the Osamu Utsumi mine and Morro do Ferro analogue study sites, Brazil
D C Holmes[1], A E Pitty[2], R Noy[1]
[1] British Geological Survey, Keyworth
[2] INTERRA/ECL, Leicestershire, UK
December 1990

TR 90-15
Chemical and isotopic composition of groundwaters and their seasonal variability at the Osamu Utsumi and Morro do Ferro analogue study sites, Poços de Caldas, Brazil
D K Nordstrom[1], J A T Smellie[2], M Wolf[3]
[1] US Geological Survey, Menlo Park
[2] Conterra AB, Uppsala
[3] Gesellschaft für Strahlen- und Umweltforschung (GSF), Munich
December 1990

TR 90-16

Natural radionuclide and stable element studies of rock samples from the Osamu Utsumi mine and Morro do Ferro analogue study sites, Poços de Caldas, Brazil

A B MacKenzie[1], P Linsalata[2], N Miekeley[3], J K Osmond[4], D B Curtis[5]
[1] Scottis Universities Research & Reactor Centre (SURRC), Glasgow
[2] New York Medical Centre
[3] Catholic University of Rio de Janeiro (PUC)
[4] Florida State University
[5] Los Alamos National Laboratory
December 1990

TR 90-17

Natural series nuclide and rare earth element geochemistry of waters from the Osamu Utsumi mine and Morro do Ferro analogue study sites, Poços de Caldas, Brazil

N Miekeley[1], O Coutinho de Jesus[1], C-L Porto da Silveira[1], P Linsalata[2], J N Andrews[3], J K Osmond[4]
[1] Catholic University of Rio de Janeiro (PUC)
[2] New York Medical Centre
[3] University of Bath
[4] Florida State University
December 1990

TR 90-18

Chemical and physical characterisation of suspended particles and colloids in waters from the Osamu Utsumi mine and Morro do Ferro analogue study sites, Poços de Caldas, Brazil

N Miekeley[1], O Coutinho de Jesus[1], C-L Porto da Silveira[1], C Degueldre[2]
[1] Catholic University of Rio de Janeiro (PUC)
[2] PSI, Villingen, Switzerland
December 1990

TR 90-19

Microbiological analysis at the Osamu Utsumi mine and Morro do Ferro analogue study sites, Poços de Caldas, Brazil

J West[1], A Vialta[2], I G McKinley[3]
[1] British Geological Survey, Keyworth
[2] Uranio do Brasil, Poços de Caldas
[3] NAGRA, Baden, Sitzerland
December 1990

TR 90-20

Testing of geochemical models in the Poços de Caldas analogue study

J Bruno[1], J E Cross[2], J Eikenberg[3], I G McKinley[4], D Read[5], A Sandino[1], P Sellin[6]
[1] Royal Institute of Technology (KTH), Stockholm
[2] AERE, Harwell, UK
[3] PSI, Villingen, Switzerland
[4] NAGRA, Baden, Switzerland
[5] Atkins ES, Epsom, UK
[6] Swedish Nuclear and Waste Management Co (SKB), Stockholm
December 1990

TR 90-21

Testing models of redox front migration and geochemistry at the Osamu Utsumi mine and Morro do Ferro analogue sites, Poços de Caldas, Brazil

J Cross[1], A Haworth[1], P C Lichtner[2], A B MacKenzi[3], L Moreno[4], I Neretnieks[4], D K Nordstrom[5], D Read[6], L Romero[4], S M Sharland[1], C J Tweed[1]
[1] AERE, Harwell, UK
[2] University of Bern
[3] Scottish Universities Research & Reactor Centre (SURRC), Glasgow
[4] Royal Institute of Technology (KTH), Stockholm
[5] US Geological Survey, Menlo Park
[6] Atkins ES, Epsom, UK
December 1990

TR 90-22

Near-field high temperature transport: Evidence from the genesis of the Osamu Utsumi uranium mine analogue site, Poços de Caldas, Brazil

L M Cathles[1], M E Shea[2]
[1] University of Cornell, New York
[2] Battelle, Chicago
December 1990

TR 90-23

Geochemical modelling of water-rock interactions at the Osamu Utsumi mine and Morro do Ferro analogue sites, Poços de Caldas, Brazil

D K Nordstrom[1], I Puigdomenech[2], R H McNutt[3]
[1] US Geological Survey, Menlo Park
[2] Studsvik Nuclear, Sweden
[3] McMaster University, Ontario, Canada
December 1990

TR 90-24

The Poços de Caldas Project: Summary and implications for radioactive waste management

N A Chapman[1], I G McKinley[2], M E Shea[3], J A T Smellie[4]
[1] INTERRA/ECL, Leicestershire, UK
[2] NAGRA, Baden, Switzerland
[3] Battelle, Chicago
[4] Conterra AB, Uppsala

TR 90-25

Kinetics of UO_2(s) dissolution reducing conditions: numerical modelling

I Puigdomenech[1], I Cass[2], J Bruno[3]
[1] Studsvik AB, Nyköping, Sweden
[2] Department of Chemical Engineering, E.T.S.E.I.B. (U.P.C.), Barcelona, Spain
[3] Department of Inorganic Chemistry, The Royal Institute of Technology, Stockholm, Sweden
May 1990

TR 90-26

The effect from the number of cells, pH and lanthanide concentration on the sorption of promethium on gramnegative bacterium (Shewanella Putrefaciens)

Karsten Pedersen[1], Yngve Albinsson[2]
[1] University of Göteborg, Department of General and Marine Microbiology, Gothenburg, Sweden
[2] Chalmers University of Technology, Department of Nuclear Chemistry, Gothenburg, Sweden
June 1990

TR 90-27

Isolation and characterization of humics from natural waters

B Allard[1], I Arsenie[1], H Borén[1], J Ephraim[1], G Gårdhammar[2], C Pettersson[1]
[1] Department of Water and Environmental Studies, Linköping University, Linköping, Sweden
[2] Department of Chemistry, Linköping University, Linköping, Sweden
May 1990

TR 90-28

Complex forming properties of natural organic acids. Part 2. Complexes with iron and calcium

James H Ephraim[1], Andrew S Mathuthu[2], Jacob A Marinsky[3]
[1] Department of Water in Environment and Society, Linköping University, Linköping, Sweden
[2] Chemistry department, University of Zimbabwe, Harare, Zimbabwe
[3] Chemistry Department, State University of New York at Buffalo, Buffalo, NY, USA
July 1990

TR 90-29

Characterization of humic substances from deep groundwaters in granitic bedrock in Sweden

C Pettersson, J Ephraim, B Allard, H Borén
Department of Water and Environmental Studies, Linköping University, Linköping, Sweden
June 1990

TR 90-30

The earthquakes of the Baltic shield

Ragnar Slunga
Swedish National Defence Research Institute
June 1990